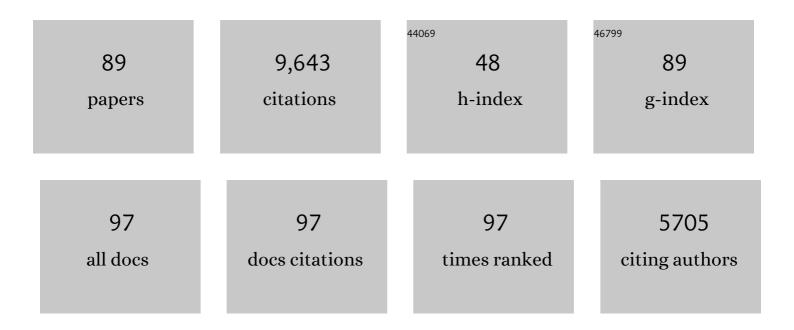
List of Publications by Year in descending order

Source: https://exaly.com/author-pdf/6435425/publications.pdf Version: 2024-02-01



IÃ:NOS SZANVI

#	Article	IF	CITATIONS
1	Coordinatively Unsaturated Al ³⁺ Centers as Binding Sites for Active Catalyst Phases of Platinum on γ-Al ₂ O ₃ . Science, 2009, 325, 1670-1673.	12.6	790
2	Excellent activity and selectivity of Cu-SSZ-13 in the selective catalytic reduction of NOx with NH3. Journal of Catalysis, 2010, 275, 187-190.	6.2	674
3	Effects of hydrothermal aging on NH3-SCR reaction over Cu/zeolites. Journal of Catalysis, 2012, 287, 203-209.	6.2	438
4	Structure–activity relationships in NH3-SCR over Cu-SSZ-13 as probed by reaction kinetics and EPR studies. Journal of Catalysis, 2013, 300, 20-29.	6.2	409
5	Selective Catalytic Reduction over Cu/SSZ-13: Linking Homo- and Heterogeneous Catalysis. Journal of the American Chemical Society, 2017, 139, 4935-4942.	13.7	380
6	CO ₂ Reduction on Supported Ru/Al ₂ O ₃ Catalysts: Cluster Size Dependence of Product Selectivity. ACS Catalysis, 2013, 3, 2449-2455.	11.2	376
7	Mechanism of CO ₂ Hydrogenation on Pd/Al ₂ O ₃ Catalysts: Kinetics and Transient DRIFTS-MS Studies. ACS Catalysis, 2015, 5, 6337-6349.	11.2	355
8	Two different cationic positions in Cu-SSZ-13?. Chemical Communications, 2012, 48, 4758.	4.1	350
9	Effects of Si/Al ratio on Cu/SSZ-13 NH3-SCR catalysts: Implications for the active Cu species and the roles of BrĀ,nsted acidity. Journal of Catalysis, 2015, 331, 25-38.	6.2	341
10	Heterogeneous Catalysis on Atomically Dispersed Supported Metals: CO ₂ Reduction on Multifunctional Pd Catalysts. ACS Catalysis, 2013, 3, 2094-2100.	11.2	310
11	Understanding ammonia selective catalytic reduction kinetics over Cu/SSZ-13 from motion of the Cu ions. Journal of Catalysis, 2014, 319, 1-14.	6.2	307
12	Current Understanding of Cu-Exchanged Chabazite Molecular Sieves for Use as Commercial Diesel Engine DeNOx Catalysts. Topics in Catalysis, 2013, 56, 1441-1459.	2.8	297
13	Effects of Alkali and Alkaline Earth Cocations on the Activity and Hydrothermal Stability of Cu/SSZ-13 NH ₃ –SCR Catalysts. ACS Catalysis, 2015, 5, 6780-6791.	11.2	235
14	Kinetic modeling and transient DRIFTS–MS studies of CO2 methanation over Ru/Al2O3 catalysts. Journal of Catalysis, 2016, 343, 185-195.	6.2	180
15	Low-Temperature Pd/Zeolite Passive NO _{<i>x</i>} Adsorbers: Structure, Performance, and Adsorption Chemistry. Journal of Physical Chemistry C, 2017, 121, 15793-15803.	3.1	178
16	Synthesis and Evaluation of Cu-SAPO-34 Catalysts for Ammonia Selective Catalytic Reduction. 1. Aqueous Solution Ion Exchange. ACS Catalysis, 2013, 3, 2083-2093.	11.2	168
17	Synthesis and evaluation of Cu/SAPO-34 catalysts for NH3-SCR 2: Solid-state ion exchange and one-pot synthesis. Applied Catalysis B: Environmental, 2015, 162, 501-514.	20.2	166
18	Characterization of Cu-SSZ-13 NH3 SCR catalysts: an in situ FTIR study. Physical Chemistry Chemical Physics, 2013, 15, 2368.	2.8	142

#	Article	IF	CITATIONS
19	NO Chemisorption on Cu/SSZ-13: A Comparative Study from Infrared Spectroscopy and DFT Calculations. ACS Catalysis, 2014, 4, 4093-4105.	11.2	139
20	On the hydrothermal stability of Cu/SSZ-13 SCR catalysts. Applied Catalysis A: General, 2018, 560, 185-194.	4.3	132
21	Following the movement of Cu ions in a SSZ-13 zeolite during dehydration, reduction and adsorption: A combined in situ TP-XRD, XANES/DRIFTS study. Journal of Catalysis, 2014, 314, 83-93.	6.2	131
22	Achieving Atomic Dispersion of Highly Loaded Transition Metals in Smallâ€Pore Zeolite SSZâ€13: Highâ€Capacity and Highâ€Efficiency Lowâ€Temperature CO and Passive NO _{<i>x</i>} Adsorbers. Angewandte Chemie - International Edition, 2018, 57, 16672-16677.	13.8	129
23	The Adsorption of NO and Reaction of NO with O2on H-, NaH-, CuH-, and Cu-ZSM-5: Anin SituFTIR Investigation. Journal of Catalysis, 1996, 164, 232-245.	6.2	123
24	Dissecting the steps of CO ₂ reduction: 1. The interaction of CO and CO ₂ with γ-Al ₂ O ₃ : an in situ FTIR study. Physical Chemistry Chemical Physics, 2014, 16, 15117-15125.	2.8	103
25	Unique Role of Anchoring Penta-Coordinated Al ³⁺ Sites in the Sintering of γ-Al ₂ O ₃ -Supported Pt Catalysts. Journal of Physical Chemistry Letters, 2010, 1, 2688-2691.	4.6	101
26	Sub-micron Cu/SSZ-13: Synthesis and application as selective catalytic reduction (SCR) catalysts. Applied Catalysis B: Environmental, 2017, 201, 461-469.	20.2	101
27	Molecular Level Understanding of How Oxygen and Carbon Monoxide Improve NO _{<i>x</i>} Storage in Palladium/SSZ-13 Passive NO _{<i>x</i>} Adsorbers: The Role of NO ⁺ and Pd(II)(CO)(NO) Species. Journal of Physical Chemistry C, 2018, 122, 10820-10827.	3.1	101
28	Optimizing Active Sites for High CO Selectivity during CO ₂ Hydrogenation over Supported Nickel Catalysts. Journal of the American Chemical Society, 2021, 143, 4268-4280.	13.7	100
29	Unraveling the mysterious failure of Cu/SAPO-34 selective catalytic reduction catalysts. Nature Communications, 2019, 10, 1137.	12.8	99
30	The effect of CO on CO2 methanation over Ru/Al2O3 catalysts: a combined steady-state reactivity and transient DRIFT spectroscopy study. Applied Catalysis B: Environmental, 2019, 256, 117791.	20.2	98
31	A Common Intermediate for N ₂ Formation in Enzymes and Zeolites: Sideâ€On Cu–Nitrosyl Complexes. Angewandte Chemie - International Edition, 2013, 52, 9985-9989.	13.8	94
32	A comparative kinetics study between Cu/SSZ-13 and Fe/SSZ-13 SCR catalysts. Catalysis Today, 2015, 258, 347-358.	4.4	94
33	Transformation of Active Sites in Fe/SSZ-13 SCR Catalysts during Hydrothermal Aging: A Spectroscopic, Microscopic, and Kinetics Study. ACS Catalysis, 2017, 7, 2458-2470.	11.2	89
34	Controlling selectivities in CO2 reduction through mechanistic understanding. Nature Communications, 2017, 8, 513.	12.8	85
35	Tomography and High-Resolution Electron Microscopy Study of Surfaces and Porosity in a Plate-like γ-Al ₂ O ₃ . Journal of Physical Chemistry C, 2013, 117, 179-186.	3.1	81
36	Palladium/Beta zeolite passive NOx adsorbers (PNA): Clarification of PNA chemistry and the effects of CO and zeolite crystallite size on PNA performance. Applied Catalysis A: General, 2019, 569, 141-148.	4.3	81

#	Article	IF	CITATIONS
37	Carboxyl intermediate formation via an in situ-generated metastable active site during water-gas shift catalysis. Nature Catalysis, 2019, 2, 916-924.	34.4	79
38	Recent advances in hybrid metal oxide–zeolite catalysts for low-temperature selective catalytic reduction of NOx by ammonia. Applied Catalysis B: Environmental, 2021, 291, 120054.	20.2	78
39	Structure of Îʿ-Alumina: Toward the Atomic Level Understanding of Transition Alumina Phases. Journal of Physical Chemistry C, 2014, 118, 18051-18058.	3.1	72
40	Stabilization of Super Electrophilic Pd ⁺² Cations in Small-Pore SSZ-13 Zeolite. Journal of Physical Chemistry C, 2020, 124, 309-321.	3.1	67
41	Revisiting effects of alkali metal and alkaline earth co-cation additives to Cu/SSZ-13 selective catalytic reduction catalysts. Journal of Catalysis, 2019, 378, 363-375.	6.2	59
42	The superior hydrothermal stability of Pd/SSZ-39 in low temperature passive NOx adsorption (PNA) and methane combustion. Applied Catalysis B: Environmental, 2021, 280, 119449.	20.2	56
43	Mechanistic insight into the passive NOx adsorption in the highly dispersed Pd/HBEA zeolite. Applied Catalysis A: General, 2019, 569, 181-189.	4.3	55
44	High temperature transition aluminas in δ-Al2O3/Î,-Al2O3 stability range: Review. Journal of Catalysis, 2021, 393, 357-368.	6.2	55
45	Environment of Metal–O–Fe Bonds Enabling High Activity in CO ₂ Reduction on Single Metal Atoms and on Supported Nanoparticles. Journal of the American Chemical Society, 2021, 143, 5540-5549.	13.7	54
46	Disordered, Sub-Nanometer Ru Structures on CeO ₂ are Highly Efficient and Selective Catalysts in Polymer Upcycling by Hydrogenolysis. ACS Catalysis, 2022, 12, 4618-4627.	11.2	54
47	Dissecting the steps of CO ₂ reduction: 2. The interaction of CO and CO ₂ with Pd/Ĵ³-Al ₂ O ₃ : an in situ FTIR study. Physical Chemistry Chemical Physics, 2014, 16, 15126-15138.	2.8	51
48	Unraveling the Origin of Structural Disorder in High Temperature Transition Al ₂ O ₃ : Structure of Î,-Al ₂ O ₃ . Chemistry of Materials, 2015, 27, 7042-7049.	6.7	51
49	Inâ€Situ Dispersion of Palladium on TiO ₂ During Reverse Water–Gas Shift Reaction: Formation of Atomically Dispersed Palladium. Angewandte Chemie - International Edition, 2020, 59, 17657-17663.	13.8	51
50	Economizing on Precious Metals in Threeâ€Way Catalysts: Thermally Stable and Highly Active Singleâ€Atom Rhodium on Ceria for NO Abatement under Dry and Industrially Relevant Conditions**. Angewandte Chemie - International Edition, 2021, 60, 391-398.	13.8	51
51	The adsorption of carbon monoxide on H-ZSM-5 and hydrothermally treated H-ZSM-5. Microporous Materials, 1996, 7, 201-218.	1.6	50
52	NO x uptake mechanism on Pt/BaO/Al2O3 catalysts. Catalysis Letters, 2006, 111, 119-126.	2.6	46
53	Unlocking the Catalytic Potential of TiO ₂ -Supported Pt Single Atoms for the Reverse Water–Gas Shift Reaction by Altering Their Chemical Environment. Jacs Au, 2021, 1, 977-986.	7.9	46
54	Effect of reaction conditions on the hydrogenolysis of polypropylene and polyethylene into gas and liquid alkanes. Reaction Chemistry and Engineering, 2022, 7, 844-854.	3.7	43

#	Article	IF	CITATIONS
55	Enhancement of high-temperature selectivity on Cu-SSZ-13 towards NH3-SCR reaction from highly dispersed ZrO2. Applied Catalysis B: Environmental, 2020, 263, 118359.	20.2	42
56	Palladium/Zeolite Low Temperature Passive NOx Adsorbers (PNA): Structure-Adsorption Property Relationships for Hydrothermally Aged PNA Materials. Emission Control Science and Technology, 2020, 6, 126-138.	1.5	38
57	Onset of High Methane Combustion Rates over Supported Palladium Catalysts: From Isolated Pd Cations to PdO Nanoparticles. Jacs Au, 2021, 1, 396-408.	7.9	37
58	Cation Movements during Dehydration and NO ₂ Desorption in a Ba–Y,FAU Zeolite: An in Situ Time-Resolved X-ray Diffraction Study. Journal of Physical Chemistry C, 2013, 117, 3915-3922.	3.1	36
59	Achieving Atomic Dispersion of Highly Loaded Transition Metals in Smallâ€Pore Zeolite SSZâ€13: Highâ€Capacity and Highâ€Efficiency Lowâ€Temperature CO and Passive NO _{<i>x</i>} Adsorbers. Angewandte Chemie, 2018, 130, 16914-16919.	2.0	34
60	Heterolytic Hydrogen Activation: Understanding Support Effects in Water–Gas Shift, Hydrodeoxygenation, and CO Oxidation Catalysis. ACS Catalysis, 2020, 10, 5663-5671.	11.2	34
61	Surface Density Dependent Catalytic Activity of Single Palladium Atoms Supported on Ceria**. Angewandte Chemie - International Edition, 2021, 60, 22769-22775.	13.8	34
62	Quantification of Highâ€Temperature Transition Al ₂ O ₃ and Their Phase Transformations**. Angewandte Chemie - International Edition, 2020, 59, 21719-21727.	13.8	28
63	Precise Identification and Characterization of Catalytically Active Sites on the Surface of γâ€Alumina**. Angewandte Chemie - International Edition, 2021, 60, 17522-17530.	13.8	26
64	Palladium/Ferrierite versus Palladium/SSZâ€13 Passive NOx Adsorbers: Adsorbateâ€Controlled Location of Atomically Dispersed Palladium(II) in Ferrierite Determines High Activity and Stability**. Angewandte Chemie - International Edition, 2022, 61, .	13.8	24
65	Elucidating the Role of CO in the NO Storage Mechanism on Pd/SSZ-13 with <i>in Situ</i> DRIFTS. Journal of Physical Chemistry C, 2022, 126, 1439-1449.	3.1	22
66	Improved thermal stability of a copper-containing ceria-based catalyst for low temperature CO oxidation under simulated diesel exhaust conditions. Catalysis Science and Technology, 2018, 8, 1383-1394.	4.1	20
67	Catalytic activation of ethylene C–H bonds on uniform d ⁸ Ir(<scp>i</scp>) and Ni(<scp>ii</scp>) cations in zeolites: toward molecular level understanding of ethylene polymerization on heterogeneous catalysts. Catalysis Science and Technology, 2019, 9, 6570-6576.	4.1	20
68	Quantitative Cu Counting Methodologies for Cu/SSZ-13 Selective Catalytic Reduction Catalysts by Electron Paramagnetic Resonance Spectroscopy. Journal of Physical Chemistry C, 2020, 124, 28061-28073.	3.1	20
69	Inâ€Situ Dispersion of Palladium on TiO ₂ During Reverse Water–Gas Shift Reaction: Formation of Atomically Dispersed Palladium. Angewandte Chemie, 2020, 132, 17810-17816.	2.0	18
70	Remarkable self-degradation of Cu/SAPO-34 selective catalytic reduction catalysts during storage at ambient conditions. Catalysis Today, 2021, 360, 367-374.	4.4	18
71	Roles of Pt and BaO in the Sulfation of Pt/BaO/Al ₂ O ₃ Lean NO <i>_x</i> Trap Materials:  Sulfur K-edge XANES and Pt L _{III} XAFS Studies. Journal of Physical Chemistry C, 2008, 112, 2981-2987.	3.1	17
72	Structure and activity of supported bimetallic NiPd nanoparticles: influence of preparation method on CO ₂ reduction. ChemCatChem, 2020, 12, 2967-2976.	3.7	17

#	Article	IF	CITATIONS
73	Tuning CO ₂ Hydrogenation Selectivity by N-Doped Carbon Coating over Nickel Nanoparticles Supported on SiO ₂ . ACS Sustainable Chemistry and Engineering, 2022, 10, 2331-2342.	6.7	17
74	Temperature-Dependent Communication between Pt/Al ₂ O ₃ Catalysts and Anatase TiO ₂ Dilutant: the Effects of Metal Migration and Carbon Transfer on the Reverse Water–Gas Shift Reaction. ACS Catalysis, 2021, 11, 12058-12067.	11.2	16
75	Precise Identification and Characterization of Catalytically Active Sites on the Surface of γâ€Alumina**. Angewandte Chemie, 2021, 133, 17663-17671.	2.0	15
76	Structural Intergrowth in δ-Al ₂ O ₃ . Journal of Physical Chemistry C, 2019, 123, 9454-9460.	3.1	14
77	On the Nature of Extra-Framework Aluminum Species and Improved Catalytic Properties in Steamed Zeolites. Molecules, 2022, 27, 2352.	3.8	12
78	Economizing on Precious Metals in Threeâ€Way Catalysts: Thermally Stable and Highly Active Singleâ€Atom Rhodium on Ceria for NO Abatement under Dry and Industrially Relevant Conditions**. Angewandte Chemie, 2021, 133, 395-402.	2.0	10
79	Designing Ceria/Alumina for Efficient Trapping of Platinum Single Atoms. ACS Sustainable Chemistry and Engineering, 2022, 10, 7603-7612.	6.7	9
80	Zeoliticâ€Imidazolate Framework Derived Intermetallic Nickel Zinc Carbide Material as a Selective Catalyst for CO ₂ to CO Reduction at High Pressure. European Journal of Inorganic Chemistry, 2021, 2021, 4521-4529.	2.0	8
81	Biomimetic CO oxidation below â~100 °C by a nitrate-containing metal-free microporous system. Nature Communications, 2021, 12, 6033.	12.8	8
82	Formation, Characterization, and Reactivity of Adsorbed Oxygen on BaO/Pt(111). Journal of Physical Chemistry C, 2010, 114, 20195-20206.	3.1	6
83	Where Does the Sulphur Go? Deactivation of a Low Temperature CO Oxidation Catalyst by Sulphur Poisoning. Catalysis Letters, 2018, 148, 1445-1450.	2.6	3
84	Quantification of Highâ€Temperature Transition Al ₂ O ₃ and Their Phase Transformations**. Angewandte Chemie, 2020, 132, 21903-21911.	2.0	3
85	Pd/FER vs Pd/SSZâ€13 Passive NOx Adsorbers: Adsorbate ontrolled Location of Atomically Dispersed Pd(II) in FER Determines High Activity and Stability. Angewandte Chemie, 0, , .	2.0	2
86	Rücktitelbild: Achieving Atomic Dispersion of Highly Loaded Transition Metals in Smallâ€Pore Zeolite SSZâ€13: Highâ€Capacity and Highâ€Efficiency Lowâ€Temperature CO and Passive NO _{<i>x</i>} Adsorbers (Angew. Chem. 51/2018). Angewandte Chemie, 2018, 130, 17152-17152.	2.0	1
87	Rücktitelbild: Surface Density Dependent Catalytic Activity of Single Palladium Atoms Supported on Ceria (Angew. Chem. 42/2021). Angewandte Chemie, 2021, 133, 23212-23212.	2.0	1
88	Crystallographic Analysis of Transition Al2O3 Phases Under the Constrains of Complex Intergrowth and Disorder. Microscopy and Microanalysis, 2020, 26, 1532-1534.	0.4	0
89	Surface Density Dependent Catalytic Activity of Single Palladium Atoms Supported on Ceria**. Angewandte Chemie, 2021, 133, 22951.	2.0	0